Taylor & Francis
Taylor & Francis Group

Computer Methods in Biomechanics and Biomedical Engineering

ISSN: 1025-5842 (Print) 1476-8259 (Online) Journal homepage: http://www.tandfonline.com/loi/gcmb20

# The effects of gastrocnemius–soleus muscle forces on ankle biomechanics during triple arthrodesis

S. Hejazi, G. Rouhi & J. Rasmussen

**To cite this article:** S. Hejazi, G. Rouhi & J. Rasmussen (2016): The effects of gastrocnemius–soleus muscle forces on ankle biomechanics during triple arthrodesis, Computer Methods in Biomechanics and Biomedical Engineering, DOI: 10.1080/10255842.2016.1206531

**To link to this article:** http://dx.doi.org/10.1080/10255842.2016.1206531

Published online: 11 Jul 2016.

COMPUTER METHODS IN BIOMECHANICS AND BIOMEDICAL ENGINEERING, 2016
http://dx.doi.org/10.1080/10255842.2016.1206531

Taylor & Francis
Taylor & Francis Group

# The effects of gastrocnemius–soleus muscle forces on ankle biomechanics during triple arthrodesis

S. Hejazi[a], G. Rouhi[a] and J. Rasmussen[b]

[a]Faculty of Biomedical Engineering, Amirkabir University of Technology, Tehran, Iran; [b]Department of Mechanical and Manufacturing Engineering, Aalborg University, Aalborg, Denmark

**ABSTRACT**

This paper presents a finite element model of the ankle, taking into account the effects of muscle forces, determined by a musculoskeletal analysis, to investigate the contact stress distribution in the tibio-talar joint in patients with triple arthrodesis and in normal subjects. Forces of major ankle muscles were simulated and corresponded well with the trend of their EMG signals. These forces were applied to the finite element model to obtain stress distributions for patients with triple arthrodesis and normal subjects in three stages of the gait cycle, i.e. heel strike, midstance, and heel rise. The results demonstrated that the stress distribution patterns of the tibio-talar joint in patients with triple arthrodesis differ from those of normal subjects in investigated gait cycle stages. The mean and standard deviations for maximum stresses in the tibo-talar joint in the stance phase for patients and normal subjects were 9.398e7 ± 1.75e7 and 7.372e7 ± 4.43e6 Pa, respectively. The maximum von Mises stresses of the tibio-talar joint for all subjects in the stance phase found to be on the lateral side of the inferior surface of the joint. The results also indicate that, in patients with triple arthrodesis, increasing gastrocnemius–soleus muscle force reduces the stress on the medial malleolus compared with normal subjects. Most of stresses in this area are between 45 and 109 kPa, and will decrease to almost 32 kPa in patients after increasing of 40% in gastrocnemius–soleus muscle force.

**ARTICLE HISTORY**
Received 28 September 2015
Accepted 23 June 2016

**KEYWORDS**
Triple arthrodesis; finite element analysis; gastrocnemius–soleus; gait analysis; AnyBody; stress distribution



## Introduction

Arthrodesis is a surgical procedure often used for treatment of advanced arthritis. Arthrodesis is prescribed for people with severe arthritis, instability, or deformity that cannot be controlled with non-surgical procedures. Many people who have arthritis, their pain can be partially relieved by rest, exercise, physiography, and other nonsurgical treatments. If these therapies could not considerably relieve the pain, arthrodesis might be prescribed.

Triple arthrodesis fuses the joints between the talus, calcaneus, and cuboid bones, thus reducing the range-of-motion of the foot and ankle complex. Not only the range of motion in fused joints changes, but also follow up after the surgery showed that fusing the joints affect the range of motion in other joints as well (Morrey & Wiedeman 1980). The change of motion pattern and the reaction moments in the fused joints can cause changes in stress distribution patterns in neighboring joints. Because of the inherent tendency of an injured ankle joint to instability, this joint rarely returns to its normal function after a serious injury. Due to changes in the biomechanics of the ankle joint after fusion, it is important to know biomechanics of the arthrodesised ankle, such as the stress distribution in a fused ankle joint.

Investigation of human's joints, such as ankle, were already studied from the clinical, mechanical, and anatomical points of view in various studies. In some of these studies mathematical models were used to investigate joints and human muscles biomechanics (Seireg & Arvikar 1973; Procter & Paul 1982). In 1973 and 1982, using mathematical models of the musculoskeletal systems, the biomechanical parameters of human body such as joints and muscle forces were obtained. In these studies the models of the lower extremity were developed, in which the forces of joints and muscles were calculated using solving the mathematical equations, and the joints' angles were calculated through using motion analysis techniques (Seireg & Arvikar 1973; Procter & Paul 1982). While these studies provided some useful information, however the mathematical equations can be solved with a variety of softwares these days. These studies were really helpful and these days these

**CONTACT** G. Rouhi grouhi@aut.ac.ir

equations can calculate by softwares and coding. Certainly for investigation of ankle biomechanics accurately, it is better to model FE musculoskeletal model of ankle which can ultimately provide accurate biomechanical models for the joints. In this case the better comparison of ankle biomechanics in normal and abnormal would be done. Some inverse dynamics studies (Robertson & Dowling 2003; Hansen et al. 2004; Moreira et al. 2013) have been conducted to determine muscle and joint torques as well as ankle forces. In Wells (1981), the ankle moment was calculated using inverse dynamics, and some other studies have calculated joint torques by mathematical modeling (Hansen et al. 2004). In Damsgaard et al. (2006) and Saraswat et al. (2010), inverse dynamic techniques were used in gait analysis to calculate the joint torques, and muscle forces were calculated using optimization methods. In Saraswat et al. (2010), a musculoskeletal model of the foot including three segments was developed, in which all muscles and ligaments of the foot were considered. In Saraswat et al. (2010) however the foot muscle force were calculated and also ankle joint is computable, but the stress distribution of bony segment in these musculoskeletal modeling is not computable. Although these musculoskeletal modeling can helpful and develop FE model of bony structure. In Perry and Burnfield (2010) muscle forces were calculated using an inverse dynamics approach, and the activation of muscles during walking was compared with EMG measurements reported in a previous study. In Moreira et al. (2013), using gait analysis in normal and pathological subjects, joint torques and joint reaction forces were obtained using inverse dynamics. Calculation of muscle forces is really time consuming because of the inverse dynamics and optimization method. There are some softwares, such as Lifemod, Opensim, and Any Body, which are based on the inverse dynamic equations and optimization method, that can calculate muscle forces and joint reaction forces. In this study AnyBody software was used for calculation of muscle forces and ankle joint forces. This Software calculates muscle force with inverse dynamic analysis and speeds up computing the muscle forces.

AnyBody, is capable of analyzing the musculoskeletal system of humans or other creatures as rigid-body in particular, the inverse dynamic analysis that resolves the fundamental indeterminacy of the muscle configuration. In this software for calculation specific muscle force, motion capture data and complete set of the boundary conditions can be given to this software and the musculoskeletal system can be fully determined the variables such as muscle and reaction forces then they can be extracted from the solution.

In Marra et al. (2015), the hip contact forces from the AnyBody models were compared to previous experimental data using Vaughan and Miami gait model (Vaughan et al. 1992; Bergmann et al. 2001), demonstrating that the simulated patterns of hip contact forces were similar to those measured with instrumented prostheses.

For a more precise evaluation, of ankle joint, in addition to musculoskeletal model of lower extremity, a reliable finite element model is required to apply the ankle muscle forces. Several studies related to the finite element model and stress distributions of the ankle joint have been published. In Anderson et al. (2004), two cadaveric ankles, one intact and one from a patient with a 4-month post-operative intra-articular fracture, were FE-modeled based on CT images, and for the stance phase of gait. The results showed that contact stresses were reduced at some distance from the fractured ankle compared to the intact cadaver model. In Anderson et al. (2007), two cadaver legs were loaded in a mechanical testing machine with a pressure sensor embedded in the ankle joint, and a FE model of ankle was developed. The results from the pressure sensors showed that the maximum stress on the tibial joint surface occurred on the lateral side. In Anderson and co-workers' study, the calculated pattern of the stresses in ankle joints were similar with the pattern of stresses that was measured using tekscan pressure sensor embedded in the ankle of cadaveric specimens (Anderson et al. 2007). The computed and measured contact stress distributions over the articular surface showed a good agreement, with correlation coefficients of 90% for one ankle and 86% for the other, in their study (Anderson et al. 2007). In Chitsazan et al. (2015), the biomechanics of the fused subtalar joint was investigated using strain gauges mounted on a cadaver tibia close to the ankle joint and by finite element models. In Chitsazan and co-worker's work, the results of FE models were in good agreements with the experimental findings using strain gauge embedded around the tibia and used for obtaining stress on the joint surface. In their study, a strong correlation was observed between the FEM and experimentally measured strains in magnitude ($R = 0.94$, $p = 0.008$).

In Cheung and Nigg (2008), an MRI-based finite element model of the foot and ankle including bony segments, ligaments and the plantar fascia embedded in a volume of encapsulated soft tissue and including a shoe was developed. The von Mises stress distributions of bones, soft tissue and ligamentous structures were obtained for the purpose of modifying design parameters of footwear (Cheung & Nigg 2008).

In most studies about stress distribution of the ankle joint (such as (Anderson et al. 2007; Chitsazan et al. 2015)), the effect of the muscle forces on the stress distribution of ankle joint was not considered in these study as mentioned above no muscle load has not been applied to cadaveric specimen. In other studies, such as Cheung and Nigg (2008), a three-dimensional FE model of human foot and ankle developed for improving design of appropriate foot wear. In this study most of foot bony segments and ligaments as

well as plantar fascia are considered. Also the load from 0 to 700 N was performed on Achilles tendon. Although this model can be helpful, the force of muscles were not calculation by optimization to apply the bony structure.

In Chen et al. (2012), a musculoskeletal finite element model of the foot was modeled and the effect of G–S muscle force was investigated on the pressure distribution of the metatarsal head of the forefoot. Their study showed that a reduction of 40% in G–S muscle force can result in dorsiflexion by 8.81° and decreased extension of the metatarsophalangeal joint by 4.65° (Chen et al. 2012). In mentioned study the force of G–S muscle were not calculation and the effects of other muscles were neglected. In most of these studies the effects of ankle muscle forces were not taken into account. Also the effect of G–S muscle on the stress distribution of ankle joint was not investigated while the G–S force can specifically effect on this stresses.

In this research, a three dimensional musculoskeletal finite element model was developed to investigate the effects of muscle forces on stress distribution in the ankle in normal and arthrodesis subjects. This work adds to state-of-the-art by including forces from all significant muscles crossing the ankle joint and by addressing three phases of the gait cycle through *in vitro* tests on normal and triple arthrodesis subjects.

## Method

Ankle muscle forces, which were derived from musculoskeletal models of gait analyses, were applied to a three-dimensional musculoskeletal FE model of ankle joint. The FE model was based on segmented CT images, and material properties of bony structures were employed. Detailed explanation of the experimental procedures and computational models are found below.

### *Gait analysis*

Five patients with bilateral triple arthrodesis (two females, three males) (age = 31.6 ± 3.2 years; mass = 66 ± 10.2 kg; height = 1.68 ± 0.106 m; BMI = 23.42 ± 3.79) were recruited. The mean duration of follow-up after surgery was 2.7 years (between 2.5 and 3 years). Furthermore, five normal subjects (two females, three males) (age = 26.4 ± 1.5 years; mass = 64.4 ± 7.8 kg; height = 1.73 ± 0.11 m; BMI = 21.59 ± 2.9) with no history of ankle disease or musculoskeletal pain volunteered for this study. All subjects provided informed consent and the experimental procedures were approved by the local ethics committee of Tehran University. Each subject performed three walking trials to obtain kinematic and kinetic parameters. Gait analysis was performed with a marker protocol according to Kadaba et al. (1990). Six cameras (Vicon, Motion System, Oxford, UK) were used to collect three-dimensional marker trajectories with a sampling rate of 100 Hz. A Kistler force plate (model: 9286BA) was used to collect ground reaction forces. EMG signals of four muscles (tibialis anterior, soleus, lateral gastrocnemius, and peroneus brevis) were recorded at 1000 Hz for all subjects during the gait cycle. An maximum voluntary contraction (MVC) test was performed according to Edward et al. (2015). The filter used for kinematic and kinetic data was chosen according to Robertson and Dowling (2003); Southgate et al. (2012); McCaw et al. (2013). The BioProc software V 3.10 (Canadian Society for Biomechanics) was used to filter data, as well as to compare the trend of muscle forces with their EMG signals. To calculate the ankle muscle forces, the marker and force plate data for each person was imported into a musculoskeletal model of the lower limb according to Vaughan (1992) that has been generated in the AnyBody Modeling System V5.3.1 (Damsgaard et al. 2006) (AnyBody Technology, Aalborg, Denmark).

### *Finite element models*

One finite element model was used for all subjects. CT data of the right foot of a healthy 47 year old man was used to create geometrically accurate 3D models of the tibia, fibula, calcaneus, cuboid, talus, and navicular bones. The segmentation was performed with Mimics, V10.01 (Materialise, Leuven, Belgium). The boundary surfaces of the bony components were processed using CATIA V5R19 (Dassault Systèmes, Paris, France) to generate surface meshes and create the corresponding 3D solid of the bones. Cartilage was modeled with Solidworks, V11, by perpendicular extrusion from the bony subchondral surfaces. Then, the solid model was imported and assembled in the finite element package ANSYS Workbench V14.5.7 (ANSYS Inc, Pittsburgh, PA, USA). The finite element model is shown in Figure 1. Phalanges were not modeled. The interactions between the cuboid, navicular,

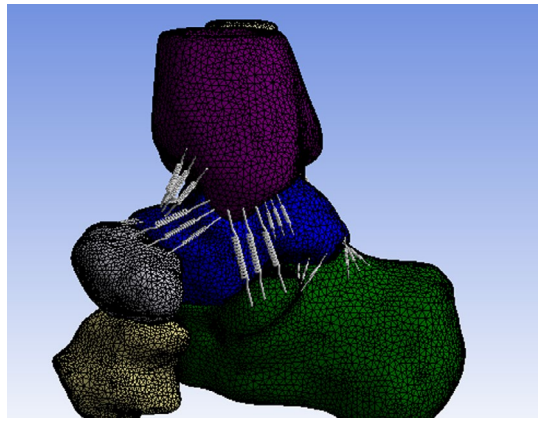

**Figure 1.** The finite element mesh of bony and ligamentous structures of the ankle joint.

talus, calcaneus, tibia, and fibula were defined as contact surfaces, which allow relative articulating movements. In all patients with triple arthrodesis, in the FE model, the talonavicular, calcaneocuboid, and talocalcaneal joints were fused. A convergence test for the discretization of the FE model was performed. The structures were meshed with a total of 183,454 ten-node tetrahedral elements with quadratic displacement fields. All ligaments were defined as tension-only elements. The ligaments across the ankle joint were modeled in the FE analysis with a single-linear spring, with the stiffness of $k = 50$ N/mm (Anderson et al. 2007). The number of these ligaments, and their insertion sites were taken from the literature (List 2009). All bony segments were idealized as homogeneous, isotropic, and linearly elastic materials except tibia which was considered orthotropic and elastic body (Ionescu et al. 2003). The Young's modulus and Poisson's ratio for the bony structures, except for the tibia, were set to 7300 MPa and 0.3, respectively (Cheung & Zhang 2005; Anderson et al. 2007). The Young's modulus and Poisson's ratio assigned to the cartilage are 12 MPa and 0.42, respectively (Anderson et al. 2007; Chitsazan et al. 2015).

The quasi-static FE simulation of the walking foot during heel-strike, midstance, and heel rise for each subject was simulated. For all subjects, the ankle muscle forces including tibialis anterior, peroneus brevis, tibialis posterior, extensor digitorum longus, extensor hallucis longus, flexor digitorum longus, and flexor hallucis longus, simulated by the AnyBody Modeling System in three phases of the gait cycle, were applied to the FE model. Sections through the distal ends of the fibula and tibia at 3.4 cm distance from the joint surfaces were fixed, and the ground reaction force vector was applied at the plantar center of pressure. Muscle forces from the musculoskeletal analysis acting along their tendons were applied by force vectors acting on the insertion point detected from the medical images (Brand et al. 1982; Delp 1990).

## Results

The simulated normalized muscle forces for four different muscles, i.e. soleus, proneus brevis, tibialis anterior, and gastrocnemius, over the gait cycle are shown in Figure 2. Interesting to note that all arthrodesis patients that participated in the gait cycle tests had an extreme initial eversion in their ankle joints (see Figure 3).

As already mentioned, the BioProc software was used to compare muscle forces calculated by AnyBody software with EMG signals. Figure 4 and Table 1 show the mean and standard deviations of EMGs of four ankle muscles, and correlation coefficients between muscle forces and their EMGs for all subjects during gait cycle, respectively.

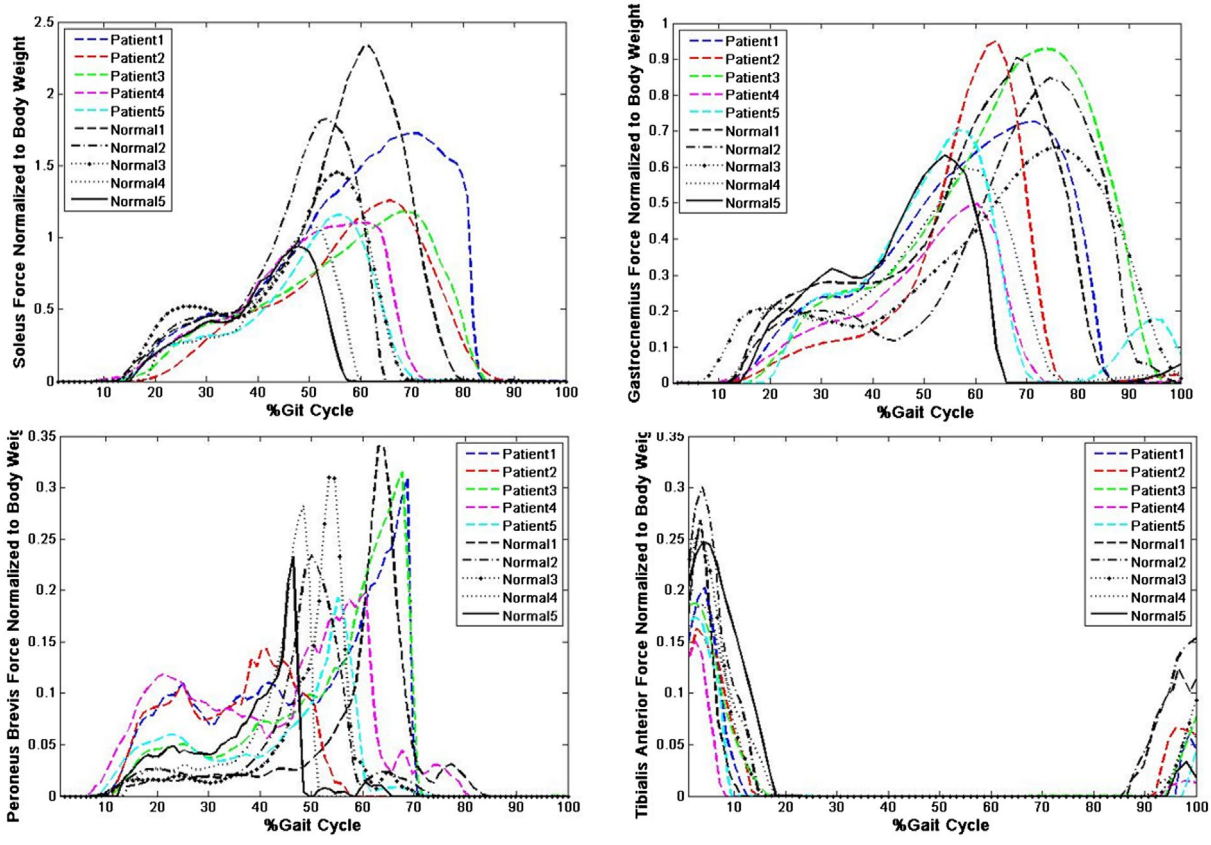


**Figure 2.** The muscle forces of soleus, gastrocnemius, peroneus brevis, and tibialis anterior that were obtained from AnyBody software.
Note: Colored lines are for patients with triple arthrodesis, and black lines are for normal subjects.

The von Mises stress distributions on the tibio-talar joint at heel strike, midstance, and heel rise for all subjects are shown in Figures 5–7, respectively. The mean and standard deviations for maximum stresses in the tibo-talar joint in the heel strike phase for patients and normal subjects are respectively 3.210e7 ± 1.7e7, 1.693e7 ± 3.56e6 Pa, and in the stance phase for patients and normal subjects respectively 9.398e7 ± 1.75e7, 7.372e7 ± 4.43e6 Pa. The maximum stresses in the tibio-talar joint in each patient are slightly lower than in the normal subjects with almost equal weight in the heel strike and midstance phases (see Figures 5 and 6). As can be seen in Figure 7, in the heel rise phase, the stress distribution in the tibio-talar joint is lower than in the midstance stage for both normal and patient subjects. The von Mises stress patterns of the tibio-talar joint for all subjects in the stance phase in the lateral side of the inferior surface of tibio-talar joint are in agreement with a previous study (Anderson et al. 2007) (see Figure 8).

Figure 9 shows the effect of the gastrocnemius (G–S) muscle force on the distributions of stress in the tibio-talar joint stress during heel rise for two selected subjects (one patient and one normal subject). With a 40% increase in G–S muscle force, the maximum von Mises stress of the tibio-talar joint increased for the normal individual while, interestingly, a reduction for the patient on the medial surface of tibio-talar joint was observed. For all patients, increasing the G–S muscle force will decrease the von Mises stress of the tibio-talar joint, especially on the medial surface of the tibio-talar joint. Increasing the G–S muscle force shifts the stress on the joint to the lateral side of the inferior surface of the joint (see Figure 9). On the medial surface of the tibia, in a patient before increasing the G–S muscle force, most of stresses in this area are between 45 and 109 kPa, and will decrease to almost 32 kPa in patients after increasing the G–S muscle force.

## Discussion and conclusions

The results of this study showed that the patterns of stress distributions in the tibio-talar joint in all patients are different from those of normal subjects in three stages of the gait cycle (see Figures 5–7). The stress level in the heel strike phase for patients is generally lower than that of normal subjects (see Figure 5). This observation can be due to the fact that some normal subjects started their gait cycles with a sharp contact in the heel strike phase while all patients started their heel strike phase more gently than normal subjects. In the midstance phase, our results for the stress distribution on the lateral side of the inferior surface of the tibio-talar joint are similar to a previous study (Anderson et al. 2007) (see Figure 8). This may be due to the fact that the ankle muscles in the stance phase are not as active as in other phases of the gait cycle, and the results in the stance phase are therefore comparable with cadaveric results tested under uniaxial load (Anderson et al. 2007). For both groups of patient and normal subjects, the maximum stresses in the tibio-talar joint are larger in the midstance phase than in the heel rise phase (see Figures 6 and 7). This can be because the heel rise phase of the right foot is simultaneous with the left foot contact, and thus some of the weight is transferred to the left foot. Good correlation between the EMG trend and the ankle muscle activations obtained from AnyBody (see Table 1) imply that the musculoskeletal gait model used by AnyBody produces valid muscle forces. In the heel rise phase with a 40% increase in G–S muscle force, the stress on the medial surface of the tibio-talar joint was interestingly reduced for patients compared with healthy subjects (see Figure 9).

The peroneus brevis forces in arthrodesis individuals were larger compared to normal subjects in the early stance phase, which is supported by the muscle's EMG patterns (see Figure 4). All participating arthrodesis patients had an extreme initial eversion of the ankle joint in the early stance phase (see Figure 3). Because one of the functions of the peroneus brevis is to evert the ankle joint, this can be the reason why the peroneus brevis muscle forces in arthrodesis patients were higher compared to normal subjects in this phase. One other reason can be this fact that the ankle requires balance about two axes and it is more likely that the peroneus has to be very active because it is maintaining equilibrium in cocontraction with another muscle (Figure 2). It seems that these patients need to reduce their extreme ankle eversion, for instance by reducing the stress on the medial surface of the tibio-talar joint. As can be seen in Figure 9, increasing G–S muscle force in these patients reduce the force on medial surface of the joint and prevent the patients from extreme eversion. Thus, therapeutic strengthening of the G–S muscle may

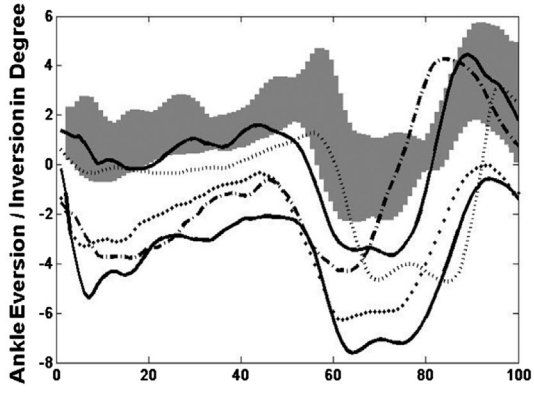


**Figure 3.** Eversion/Inversion of ankle joint.
Note: Gray band is mean plus and minus one standard deviation for normal subjects, and the lines are for patients with triple arthrodesis.

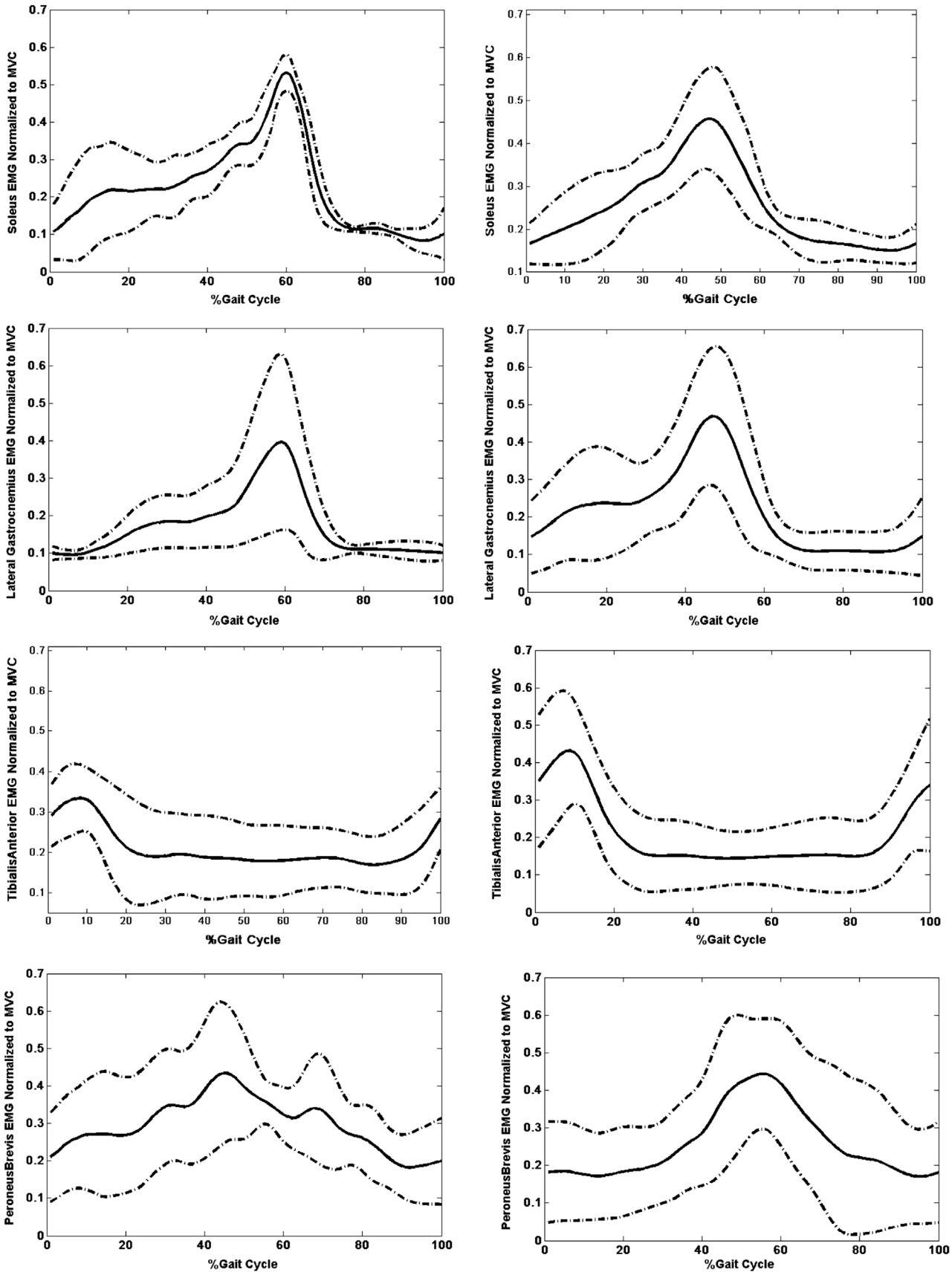


**Figure 4.** The mean and standard deviation of muscle activities (EMG signal normalized to a MVC) for the subjects of (a) patients with triple arthrodesis, and (b) normal subjects.

**Table 1.** The means and standard deviations of the correlation coefficients between muscle forces derived by AnyBody and their EMGs calculated by BioProc software for patients with triple arthrodesis and for normal subjects.

| | Correlation coefficients | |
|---|---|---|
| Muscle's name | Patients | Controls |
| Soleus | 0.89 ± 0.06 | 0.92 ± 0.03 |
| Gastrocnemius–soleus | 0.90 ± 0.03 | 0.94 ± 0.03 |
| Peroneus brevis | 0.76 ± 0.07 | 0.85 ± 0.05 |
| Tibialis anterior | 0.90 ± 0.05 | 0.92 ± 0.02 |

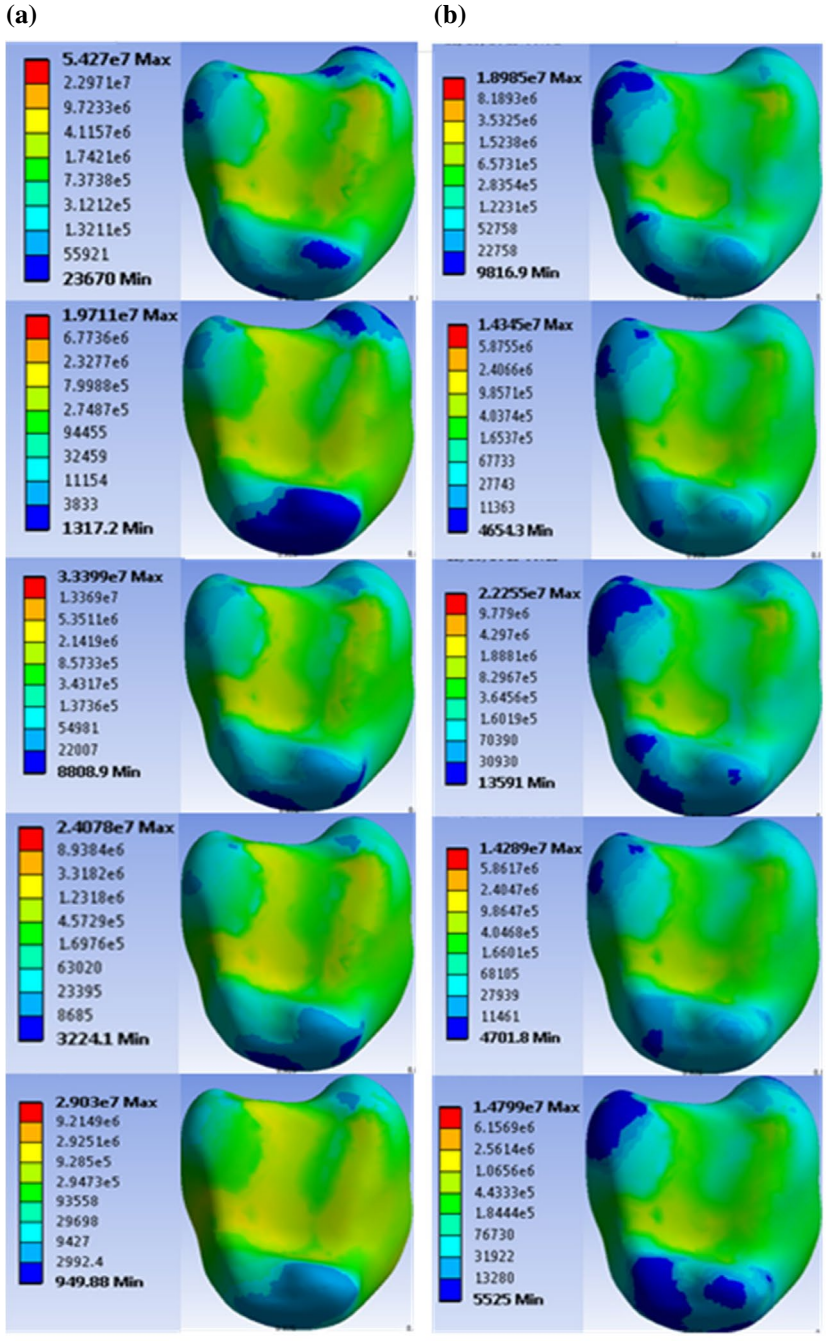


**Figure 5.** The distribution of von Mises stress of tibio-talar joint at heel strike for (a) normal subjects, and (b) patients with triple arthrodesis. The result of the ankle stress distribution for each patient subject, is placed opposite of the normal subject figure which had almost the same weight.
Note: Units are in Pascal (Pa).

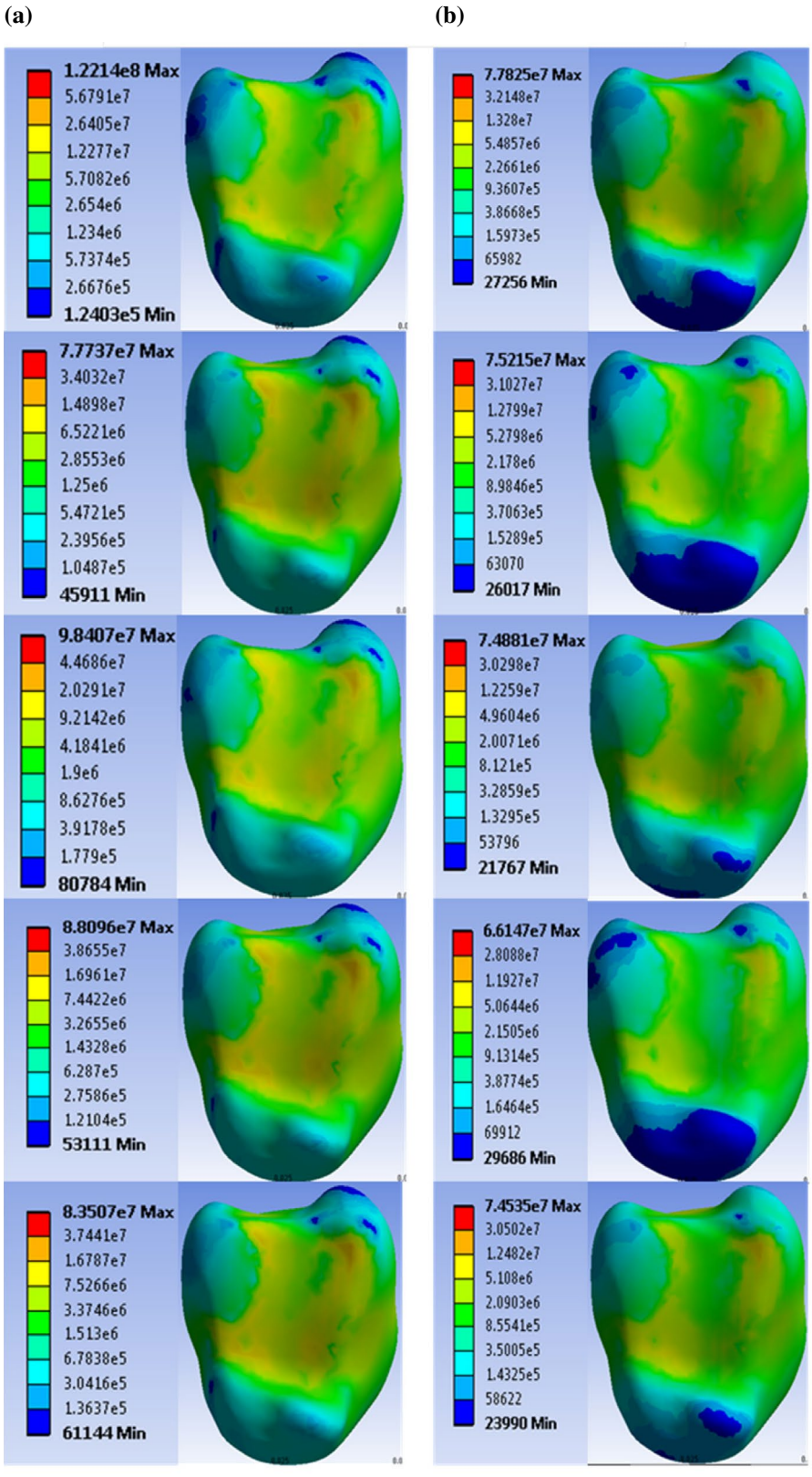


**Figure 6.** The distributions of von Mises stress of tibio-talar joint in midstance for (a) normal subjects, (b) patients with triple arthrodesis. The result of the ankle stress distribution for each patient subject, is placed opposite of the normal subject figure which had almost the same weight.
Note: Units are in Pascal (Pa).

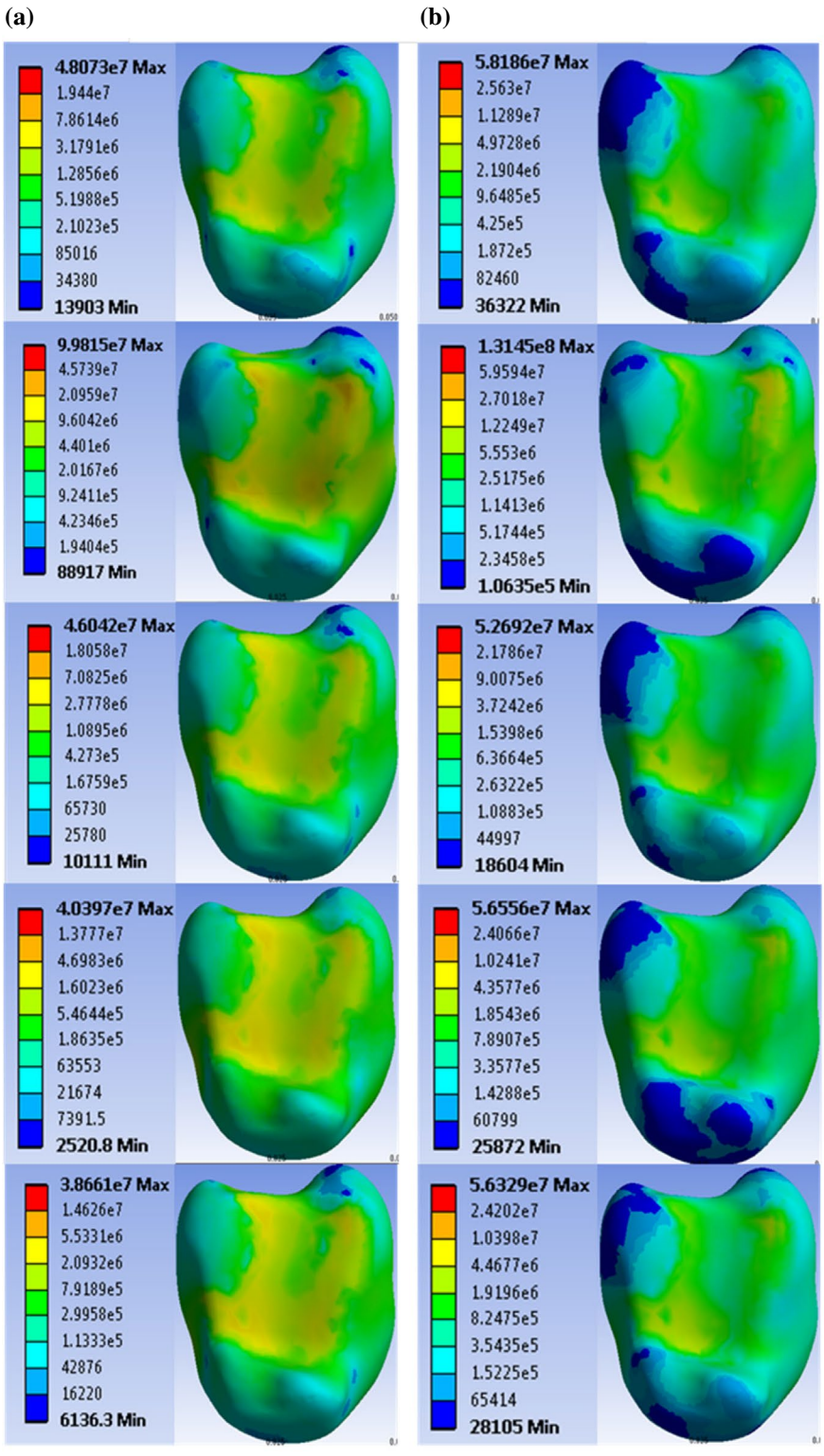


**Figure 7.** The distributions of von Mises stress of tibio-talar joint in heel rise for (a) normal subjects (b) patients with triple arthrodesis. The result of the ankle stress distribution for each patient subject, is placed opposite of the normal subject figure which had almost the same weight.

Note: Units are in Pascal (Pa).

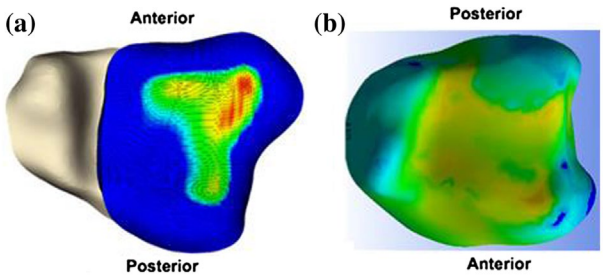


**Figure 8.** (a) The distributions of von Mises stress in the tibio-talar joint (for the left foot; Anderson et al. 2007), (b) results of this study for the stress distribution in tibio-talar joint in normal subjects in the stance phase for the right foot.

be an important rehabilitation strategy and can reduce ankle eversion (Figure 9).

There were some limitations in this study, such as in the musculoskeletal model, the foot was considered as one rigid segment such that intrincic biomechanical effects of the arthrodesis carrying over into the muscles crossing the ankle joint are not considered. Another limitation of this work was to employ just one CT image for all subjects, even though in finite element models angles of bony foot segments and boundary conditions were considered for each subject individually. Moreover, the finite element model disregarded the phalanges and the metatarsal joints. Even though metatarsal joints were disregarded in the FE model, considering the phalanges can improve this model. Another limitation of this work is the deference between the age of the participants in the experiment. As another limitation of this work, it should be noted that even though the musculoskeletal model takes inertia forces into account, the FE model works under quasi-static assumptions. This limitation cannot likely cause large errors, but future studies can investigate the effects of considering dynamic effects into the entire model.

In this research, a three dimensional musculoskeletal finite element model was developed by taking into account the effects of muscle forces in bony structure of ankle joint to investigate the contact stress distribution in the tibio-talar joint in patients with triple arthrodesis and in normal ankle joints. The FE model of bony structure of ankle which was used in this study was validated with experimental data of cadaver testing (Chitsazan et al. 2015). Furthermore, the total ankle forces in musculoskeletal FE model, were compared with the AnyBody's results for each subject. The total ankle reaction forces calculated by the FE model developed in this study, as well as the reaction forces computed by AnyBody software showed a good agreement (see Table 2). The method's ability to simulate stress distributions on the articulating surfaces of the ankle joint complex can have several important applications such as development of surgical procedures and design of artificial joints, and as such has the potential to be used by device manufacturers, physiotherapists and rehabilitation professionals to increase the quality of life of arthrodesis patients. Finally, the presented workflow of musculoskeletal forces to finite element models can be extended to other synovial joints, such as the knee, elbow,

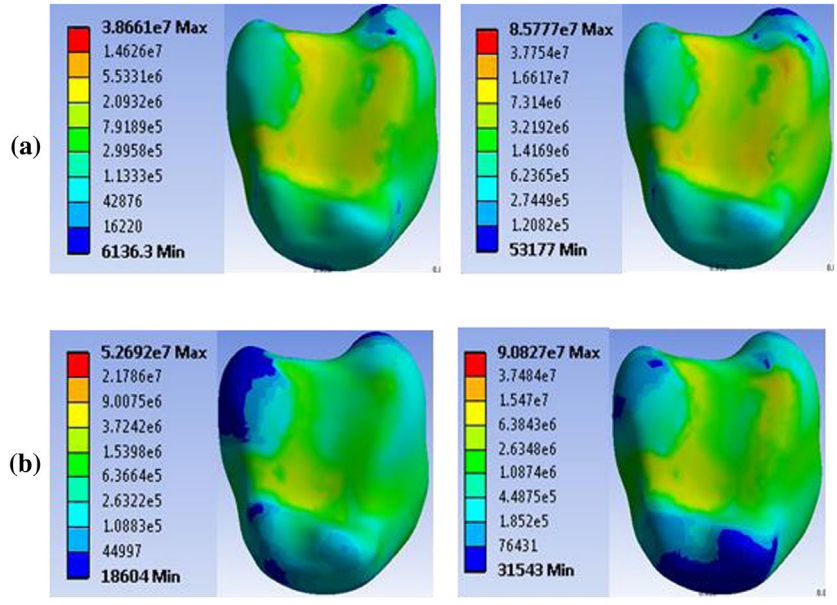


**Figure 9.** The effect of increasing the G–S muscle force (a 40% increase) on distribution of von Mises stress in tibio-talar joint in heel-rise phase of the gait cycle. Right figures show the effect of increasing the G–S muscle force on distributions of stress in tibio-talar joint in (a) normal subjects, (b) patients with triple arthrodesis.
Note: Units are in Pascal (Pa).

**Table 2.** The means and standard deviations of the total ankle reaction forces calculated by two methods including: musculoskeletal FE model and inverse dynamic process (AnyBody software) in heel strike, mid stance, and heel rise for both normal subjects and patients with triple arthrodesis.

| | Ankle reaction forces (N) | | | | | |
|---|---|---|---|---|---|---|
| | Patients | | | Controls | | |
| Method employed | Heel strike | Mid-stance | Heel rise | Heel strike | Mid-stance | Heel rise |
| Musculoskeletal FE Model | 282.79 ± 57.08 | 670.32 ± 72.88 | 983.29 ± 25.39 | 434.61 ± 63.91 | 704.01 ± 72.49 | 1033.8 ± 60.55 |
| Musculoskeletal modeling using AnyBody software | 312 ± 53.17 | 700.65 ± 61.45 | 1016.2 ± 53.76 | 404.55 ± 45.65 | 722.43 ± 67.52 | 1180.32 ± 42.23 |

and hip for investigation of a number of orthopedic conditions related to these joints.

## Acknowledgements

We would like to appreciate those who have participated in gait analysis tests. The first author also thanks Dr. G.R. Robertson for his kind support. Also we wish to thank the staff of the Ergonomics Laboratory of Iran University of Rehabilitation Sciences, and Amirkabir University of Technology.

## Disclosure statement

No potential conflict of interest was reported by the authors.

## References

Anderson, DD, Grosland NM, Brown TD. 2004. Investigating chronic stress exposure following intra-articular fracture using a finite element model of the ankle. Paper presented at: The 5th Combined Meeting of the Orthopaedic Research Societies of Canada, USA, Japan and Europe, Banff, Canada, October 11.

Anderson DD, Goldsworthy JK, Li W, Rudert MJ, Tochigi Y, Brown TD. 2007. Physical validation of a patient-specific contact finite element model of the ankle. J Biomech. 40:1662–1669.

Bergmann G, Deuretzbacher G, Heller M, Graichen F, Rohlmann A, Strauss J, Duda GN. 2001. Hip contact forces and gait patterns from routine activities. J Biomech. 34:859–871.

Brand RA, Crowninshield RD, Wittstock CE, Pedersen DR, Clark CR, Krieken FMV. 1982. A model of lower extremity muscular anatomy. J Biomech Eng. 104:304–310.

Chen W, Shim VPW, Lee T. 2012. Influence of gastrocnemius–soleus muscle force on sub-MTH load distribution. J Foot Ankle Res. 5:1–2.

Cheung JT, Nigg BM. 2008. Clinical applications of computational simulation of foot and ankle. Sports Orthop Traumatol. 23:264–271.

Cheung JTM, Zhang M. 2005. A 3-dimensional finite element model of the human foot and ankle for insole design. J Arch Phys Med Rehabil. 86:353–358.

Chitsazan A, Rouhi G, Abbasi S, Pezeshki M, Tavakoli A. 2015. Assessment of stress distribution in ankle joint: simultaneous application of experimental and finite element methods. Int J Exp Comput Biomech. 3:45–61.

Damsgaard M, Rasmussen J, Christensen ST, Surma E, de Zee MD. 2006. Analysis of musculoskeletal systems in the AnyBody modeling system. J Simul Model Pract Th. 14:1100–1111.

Delp, SL. 1990. Surgery simulation: a computer graphics system to analyze and design musculoskeletal recon-structions of the lower limb. Stanford (CA): Stanford University.

Edward, DF, Iazzetti J, Pbrotto OA, Mormson D. 2015. Anatomical guide for the electromyographer: the limbs and trunk. 5th ed. Charles C Thomas.

Hansen AH, Childress DS, Miff SC, Gard SA, Mesplay KP. 2004. The human ankle during walking: implications for design of biomimetic ankle prostheses. J Biomech. 37:1467–1474.

Ionescu, I., Conway, T., Schonning, A., Almutairi, M., Nicholson DW. 2003. Solid modeling and static finite element analysis of the human tibia. Paper presented at: The Summer Bioengineering Conference, Key Biscayne, Florida.

Kadaba MP, Ramakrishnan HK, Wootten ME. 1990. Measurement of lower extremity kinematics during level walking. J Orthop Res. 8:383–392.

List RB. 2009. Joint kinematics of unconstrained ankle arthropelasties. ETH Zurich.

Marra MA, Vanheule V, Fluit R, Koopman BHFJM, Rasmussen J, Verdonschot N, Andersen MS. 2015. A subject-specific musculoskeletal modeling framework to predict in vivo mechanics of total knee arthroplasty. J Biomech Eng. 137:734–741.

McCaw ST, Gardner JK, Stafford LN, Torry MR. 2013. Filtering ground reaction force data affects the calculation and interpretation of joint kinetics and energetics during drop landings. J Appl Biomech. 29:804–809.

Moreira, P., Lugrís U., Cuadrado J., Flores P. 2013. Biomechanical models for human gait analyses using inverse dynamics formulation. Paper presented at: The 5th Portuguese Biomechanics Congress, Espinho, Portugal, February 8–9.

Morrey BF, Wiedeman GP. 1980. Complications and long-term results of ankle arthrodeses following trauma. J Bone Joint Surg. 62:777–784.

Perry, J, Burnfield, JM. 2010. Gait analysis: normal and pathologic function. 2nd ed. New Jersey: Slack Incorporated.

Procter P, Paul JP. 1982. Ankle joint biomechanics. J Biomech. 15:627–634.

Robertson GE, Dowling JJ. 2003. Design and responses of Butterworth and critically damped digital filters. J Electromyogr Kinesiol. 13:569–573.

Saraswat P, Andersen MS, MacWilliams BA. 2010. A musculoskeletal foot model for clinical gait analysis. J Biomech. 43:1645–1652.

Seireg A, Arvikar RJ. 1973. A mathematical model for evaluation of forces in lower extremeties of the musculo-skeletal system. J Biomech. 6:313–326.

Southgate DFL, Cleather DJ, Weinert-Aplin RA, Bull, AMJ. 2012. The sensitivity of a lower limb model to axial rotation offsets and muscle bounds at the knee. J Eng Medicine. 226:660–669.

Vaughan CL, Davis BL, Connor JCO. 1992. Dynamics of human gait. 2ed ed. Mills Litho, Cape Town: Kiboho.

Wells R. 1981. The projection of the ground reaction force as a predictor of internal joint moments. J Bull Prosthet Res. 18:15–19.